

Electrons in a diode: some new perspectives on the Child-Langmuir law and other foundational theories



Y. Y. Lau

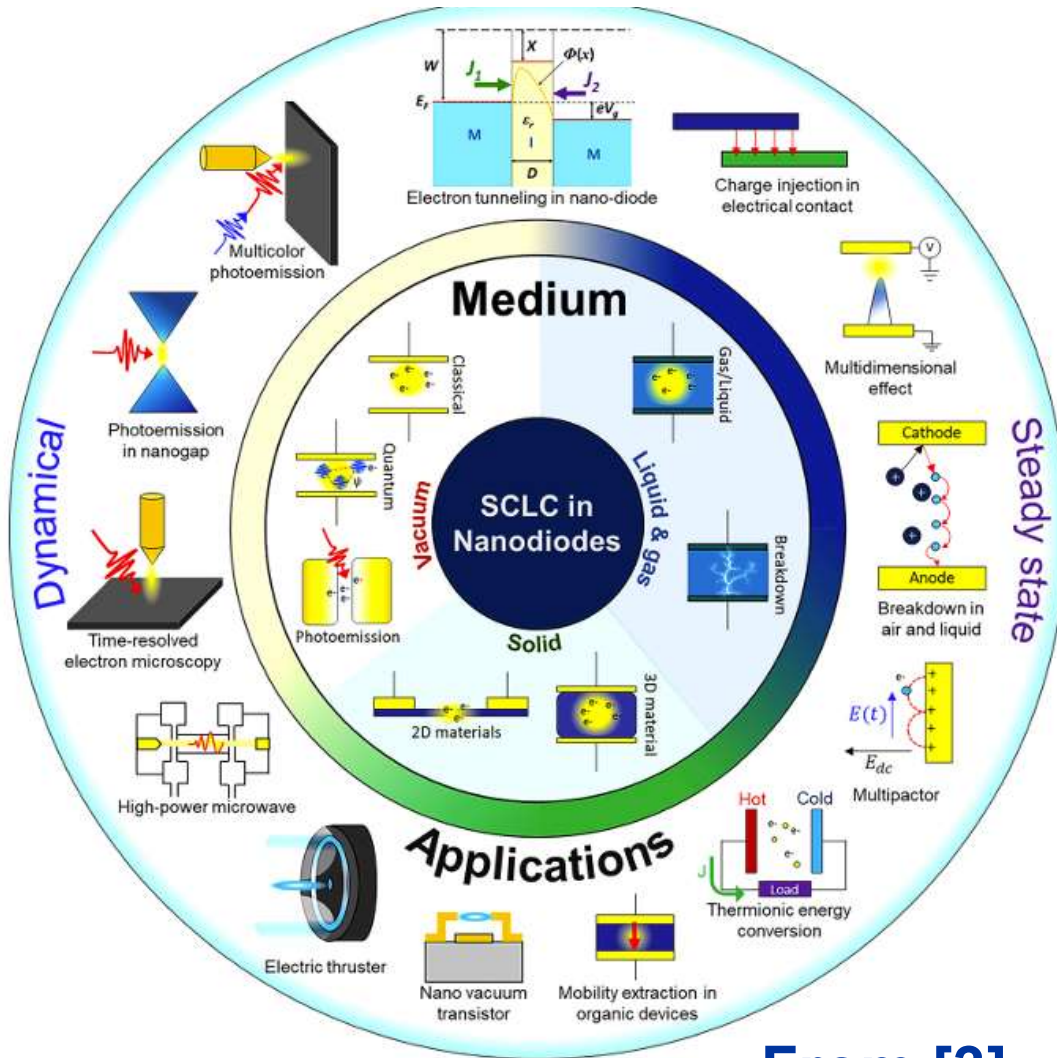
**Department of Nuclear Engineering and Radiological Sciences
University of Michigan, Ann Arbor**

Plenary Paper

**2024 IEEE IVEC/IVESC Joint Conference
Monterey, CA**

April 24, 2024

Work supported by AFOSR, DARPA, ONR, and L3Harris



Physics of Diodes

[1] P. Zhang, Á. Valfells, L. K. Ang, J. W. Luginsland, and Y. Y. Lau, “100 years of the physics of diodes,” *Applied Physics Reviews*, vol. 4, p. 011304 (2017).

[2] K. L. Jensen, *Introduction to the physics of electron emission*, Wiley (2018).

[3] P. Zhang, Y. S. Ang, A. L. Garner, Á. Valfells, J. W. Luginsland, and L. K. Ang, “Space-charge limited current in nanodiodes: Ballistic, collisional and dynamic effects,” *J. Applied Physics*, vol. 129, p. 100902 (2021).

From [3]



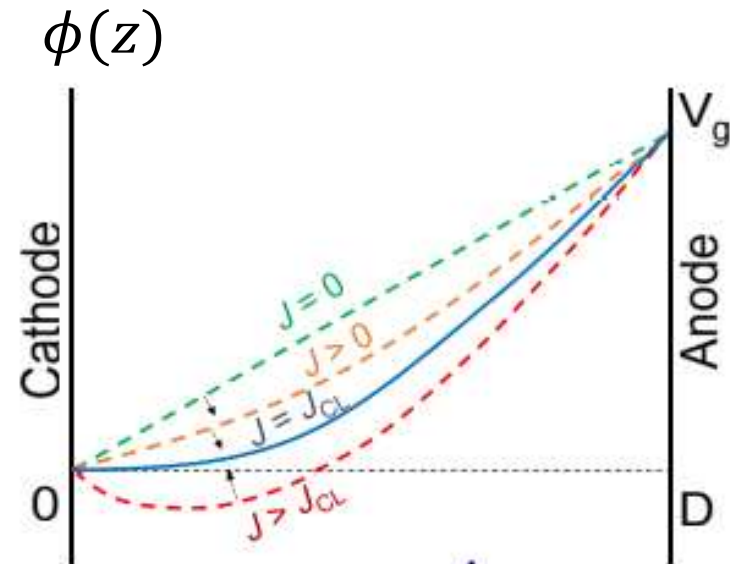
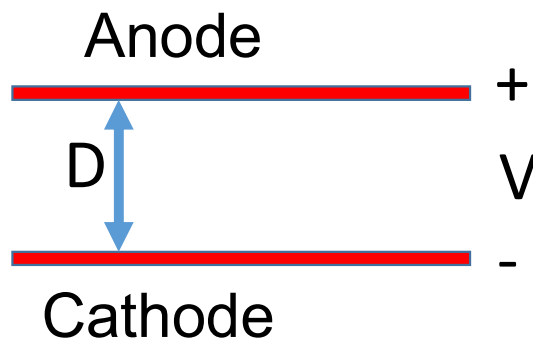
This Talk: What is new in

Child-Langmuir Law?

Ramo-Shockley Theorem?

Brillouin Flow?

Classical (1D) Child-Langmuir Law



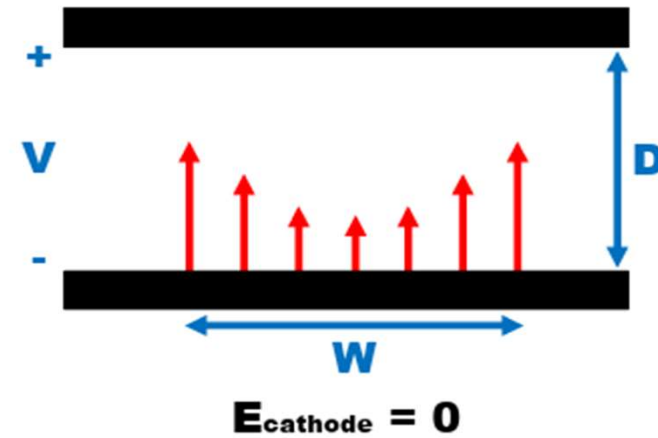
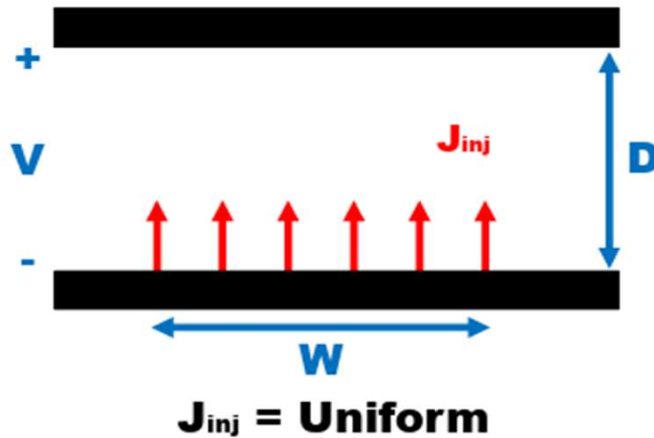
$$J_{CL} = \frac{4\sqrt{2}}{9} \epsilon_0 \left(\frac{e}{m}\right)^{1/2} \frac{V^{3/2}}{D^2} = \text{maximum current density}$$

Note: J_{CL} is independent of the cathode material, cathode temperature, or emission mechanism. It is a constraint set by the Poisson equation.

2-D Child-Langmuir Law

Emission Over a Finite Stripe (W)

Two Models



(Space-charge-limited emission)

$$\frac{J(2)}{J_{CL}} \cong 1 + 0.32 \times \frac{D}{W}, \quad 0.1 < \frac{W}{D} < \infty$$

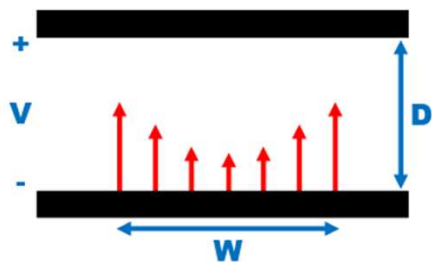
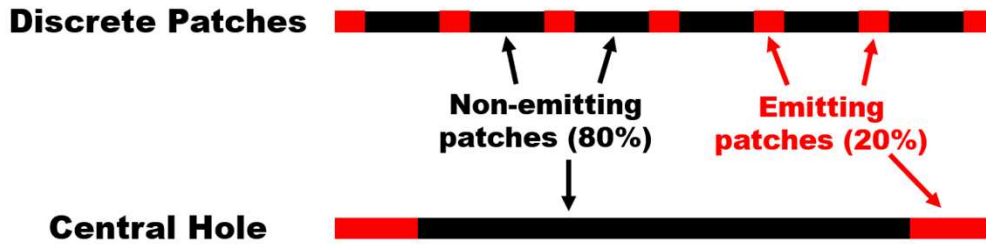
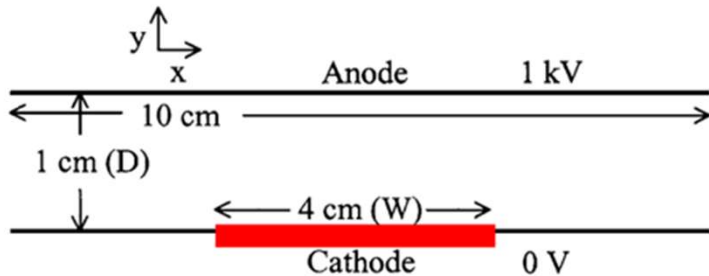
Luginsland, Lau, Gilgenbach, PRL 77, 4668 (1996)
Lau, PRL 87, 278301 (2001)

Umstattd, Luginsland, PRL 87, 145002 (2001)

(Insensitivity to B noted in both models)

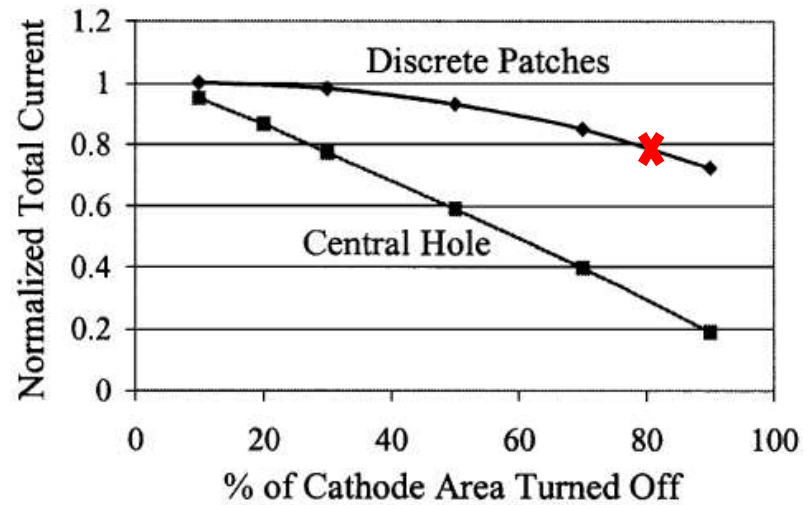
2-D Child-Langmuir Law (2)

Space-charge-limited emission over a finite stripe (W)



$(E_{\text{cathode}} = 0)$

Active Emission Area Effect on Total Current

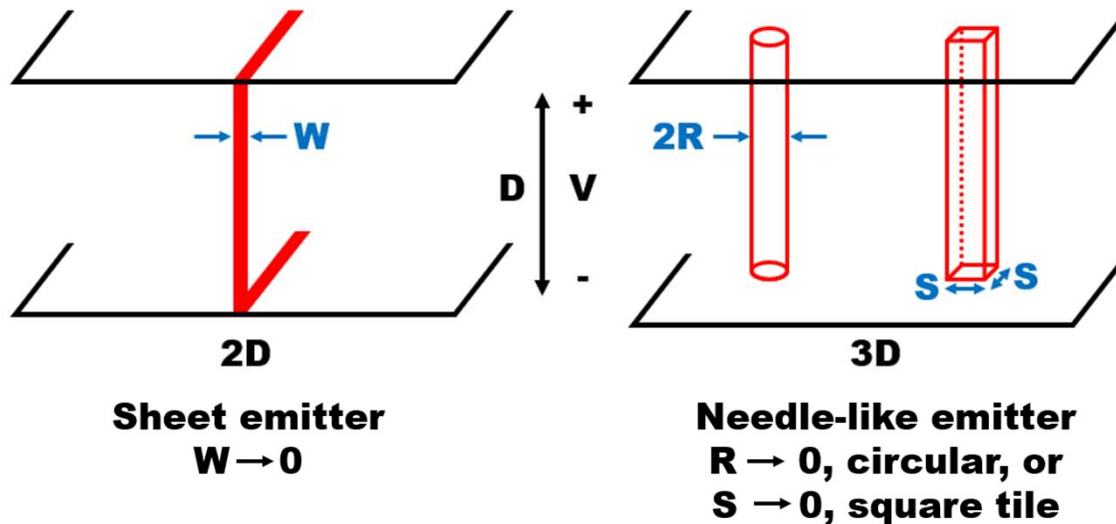


Note:

- (1) High current at the emission edge
- (2) Even with 80% cathode turned off (X), i.e., only 20% of cathode emitting, can produce 80% of the total anode current as if entire cathode were emitting.

R. Umstattd and J. Luginsland, Phys. Rev. Lett., vol. 87, p. 145002, 2001

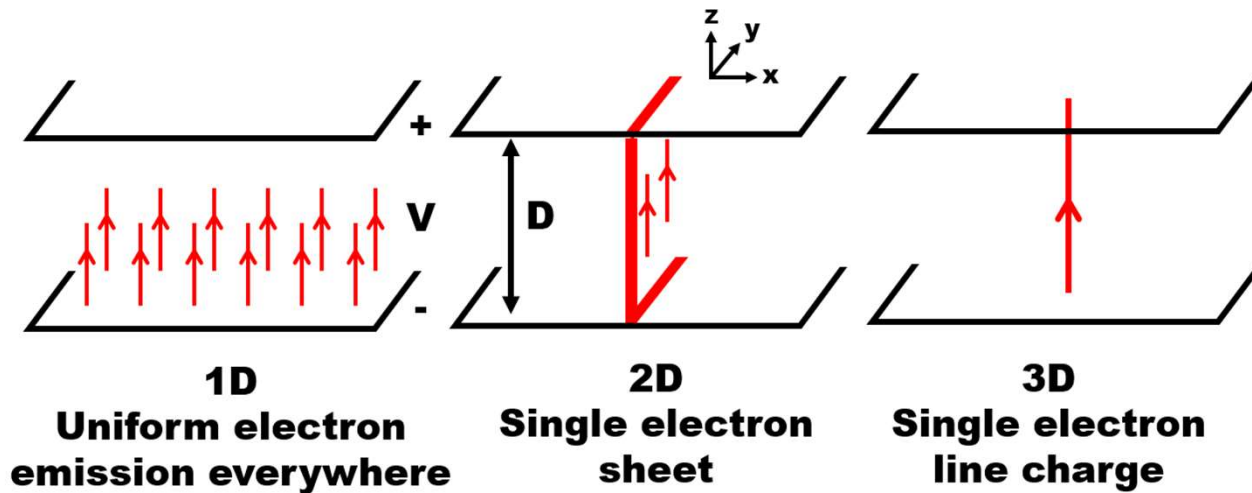
Novel Child-Langmuir Law in 2D and 3D in the limit W , R , and S approaching zero



The limiting current in these two geometries was formulated in terms of an integral equation and solved iteratively, assuming a monoenergetic electron injection energy, E_{inj} .

Y. Y. Lau, D. Li, and D. Chernin, *Phys. Plasmas* 30, 093104 (2023)
D. Chernin, D. Li, and Y. Y. Lau, *Phys. Plasmas* 31, 022103 (2024)

Child-Langmuir Law in 1D, 2D, & 3D



$$J = K_1$$

$$J = K_2 \delta(x)$$

$$J = K_3 \delta(x) \delta(y)$$

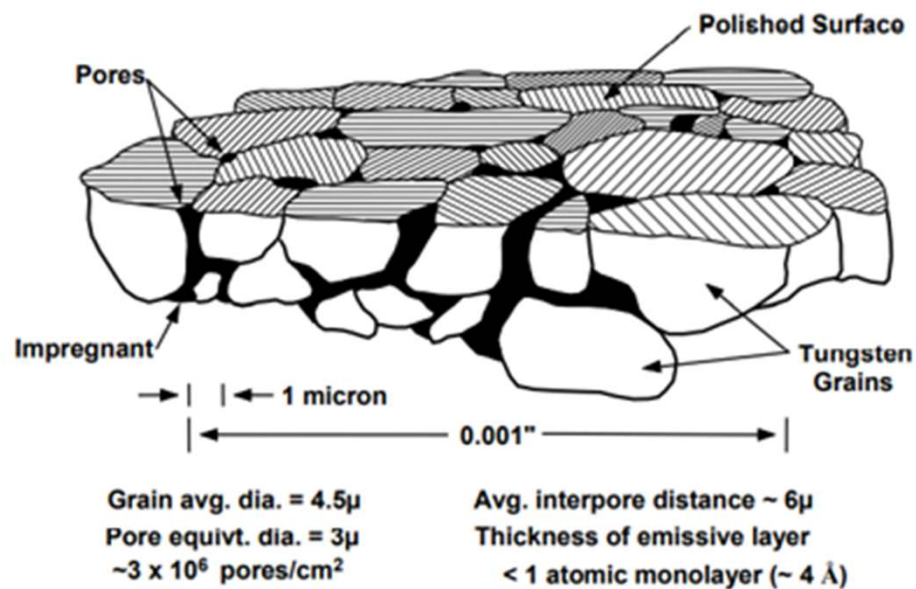
$$K_1 = J_{CL} \times \left[(1 + \Delta)^{1/2} + \Delta^{1/2} \right]^3 \equiv J_{CL\text{-Jaffe}}, \quad \Delta = E_{inj}/eV \quad \text{G. Jaffe, Phys. Rev. 65, 91 (1944)}$$

$$K_2 \cong J_{CL} \times D \times [3.302 \times \Delta^{0.5274}], \quad 0 < \Delta < 0.01 \quad \text{(unexpected result)}$$

$$K_3 = 0, \quad \text{All } \Delta \quad \text{(also an unexpected result)}$$

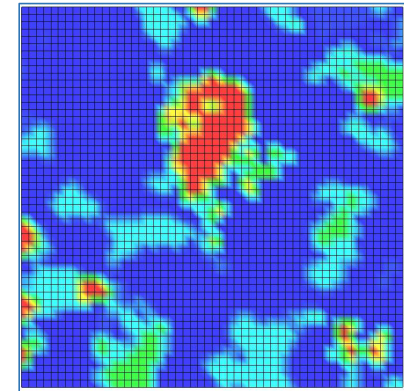
$$\text{Y. Y. Lau, D. Li, and D. Chernin, Phys. Plasmas 30, 093104 (2023)}$$

Thermionic Cathodes



Graph from A. S. Gilmour

Work Function Distribution Measurements

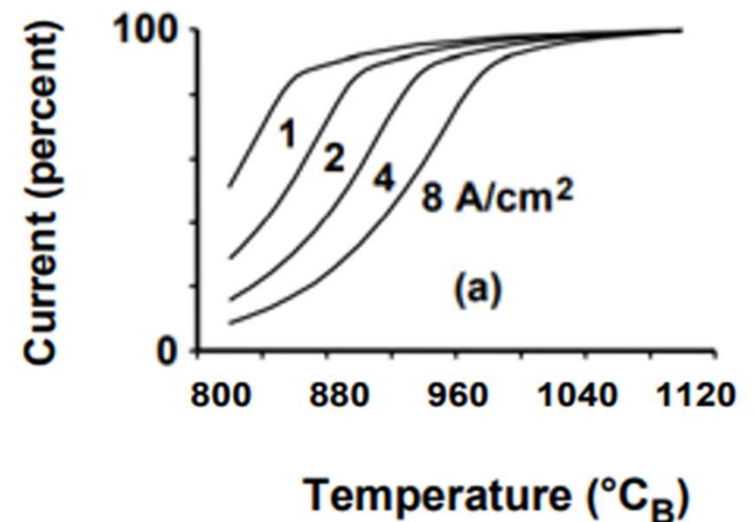


D. Chen, R. Jacobs, V. Vlahos, D. Morgan, and J. Booske, "Statistical model of non-uniform emission from polycrystalline tungsten cathodes," IVEC (Busan, S. Korea, 2019); Phys. Rev. Applied **18**, 054010 (2022).

Miram Curve* (J_{anode} vs T plot)



- Miram curves show transition from temperature limited to space charge limited regimes. Operation is always near the “knee”.
- Life of thermionic cathode is highly dependent on operating temperature; operation at 100°C lower may extend cathode life by an order of magnitude!
- Knee on Miram curve is usually much broader than 1D theory indicates. Physical reasons for shape of the knee is an outstanding question. Reason: Child-Langmuir law is independent of cathode properties.



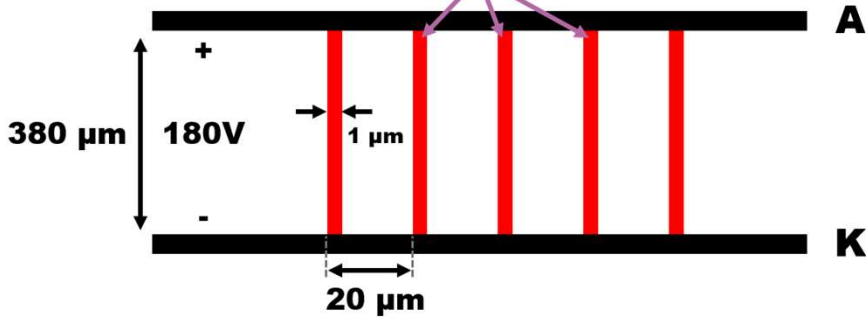
Graph from A. S. Gilmour

*M. J. Cattelino, G. V. Miram, and W. R. Ayers, IEDM Tech. Dig., pp. 36–39 (1982).

Thermionic Emission on Periodic Electron Sheets of Finite Thickness [1]



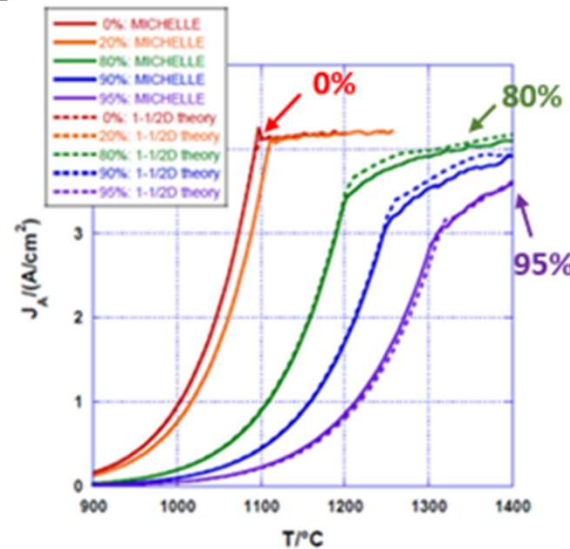
Periodic electron sheets



Note: In this example, 95% of cathode is non-emitting.

“1-1/2 D” theory: Assume $B = \infty$
 MICHELLE: Assume $B = 0$

Transverse motion unimportant to Miram curve.



1-D Child-Langmuir law is always observed at high T, even if significant fraction of area non-emitting.

[1] D. Chernin, Y. Y. Lau, J. J. Petillo, S. Ovtchinnikov, D. Chen, A. Jassem, R. Jacobs, D. Morgan, J. H. Booske, “Effect of nonuniform emission on Miram curves,” IEEE Trans. Plasma Sci. 48, 146 (2020).

[This paper won the 2023 Best Paper Award of the IEEE Trans. Plasma Sci.]

2-1/2D Model Formulation [2]

- Includes emission nonuniformity in $J_{RD}(x, y)$ through work function $\phi(x, y)$

$$J_{RD}(x, y) = AT^2 e^{-\phi(x, y)/kT}$$

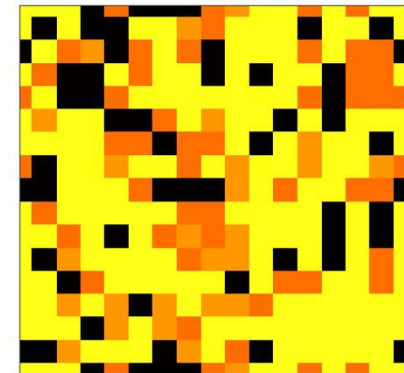
$$f(x, y, z, v_z) = \frac{J_{RD}(x, y)}{v_{th}^2} \exp\left(-\frac{mv_z^2/2 + qV(x, y, z)}{kT}\right)$$

- Solves Poisson & Vlasov equations in 2D

$$\nabla^2 V(x, y, z) = \frac{1}{\epsilon_0 v_{th}} \sqrt{\frac{\pi}{2}} J_{RD}(x, y) e^{-q(x, y, z)/kT} \operatorname{erfc}\left(\frac{v_{min}(x, y, z)}{\sqrt{2}v_{th}}\right)$$

- Periodic boundary conditions in x and y (cosine transform)

$$V_{ij}(z) = \frac{4}{N_x N_y} \sum_{l=0}^{N_x-1} \sum_{m=0}^{N_y-1} \tilde{V}_{lm}(z) \times \cos\left(\frac{2\pi l x_i}{p_x}\right) \cos\left(\frac{2\pi m y_j}{p_y}\right)$$



Note: Black tiles are non-emitting

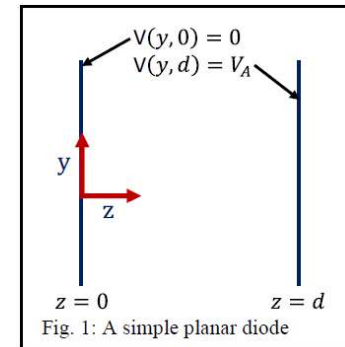
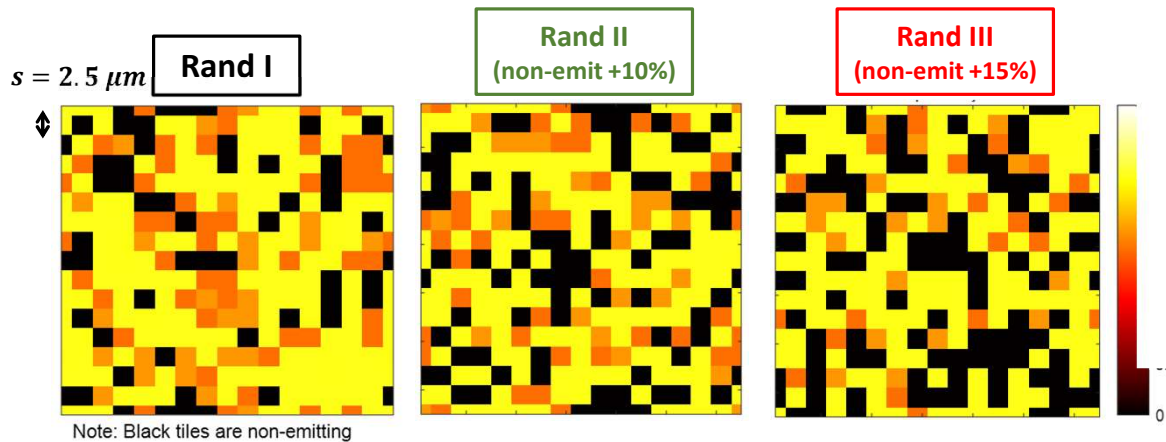
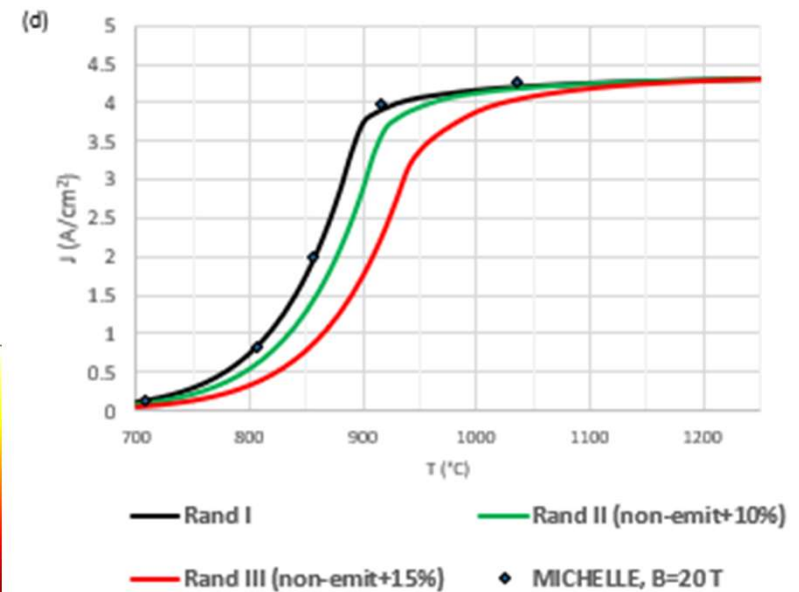


Fig. 1: A simple planar diode

[2] A. Jassem, D. Chernin, J. J. Petillo, Y. Y. Lau, A. Jensen, S. Ovtchinnikov, "Analysis of Anode Current From a Thermionic Cathode With a 2-D Work Function Distribution," IEEE Trans. Plasma Sci. 49, 749 (2021).

Validation of MICHELLE and 2-1/2D Model and Effect of higher proportion of non-emitting regions

Work Function [eV]	Experiment [1]	Rand I	Rand II	Rand III
1.61	18.54	17.97	12.89	7.42
1.79	10.32	9.77	8.59	7.42
2.3	10.99	9.38	11.33	11.33
2.31	37.69	43.75	37.50	37.11
10 (non-emitting)	22.46	19.14	29.69	36.72



[2] A. Jassem, D. Chernin, J. J. Petillo, Y. Y. Lau, A. Jensen, S. Ovtchinnikov, "Analysis of Anode Current From a Thermionic Cathode With a 2-D Work Function Distribution," IEEE Trans. Plasma Sci. 49, 749 (2021).

Contributions from WF Regions

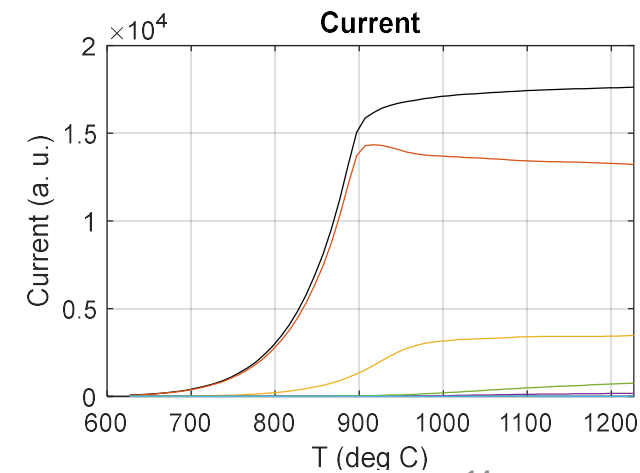
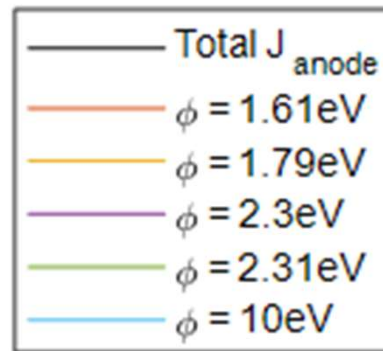
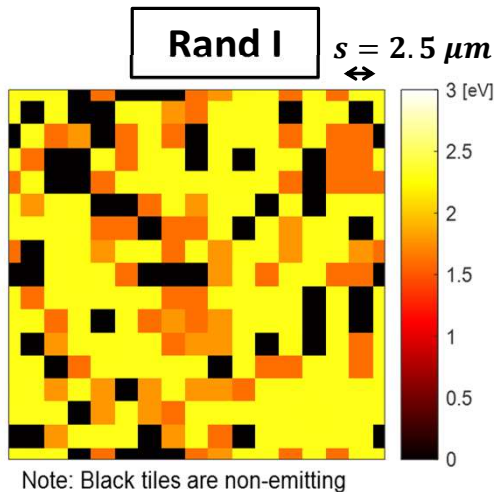
Rand I

(Random distribution based on exp. data)



- Current density contributed by the 1.61eV tiles is almost $5 \times J_{SCL}$ ($J_{SCL} \sim 4.2 \text{ A/cm}^2$)

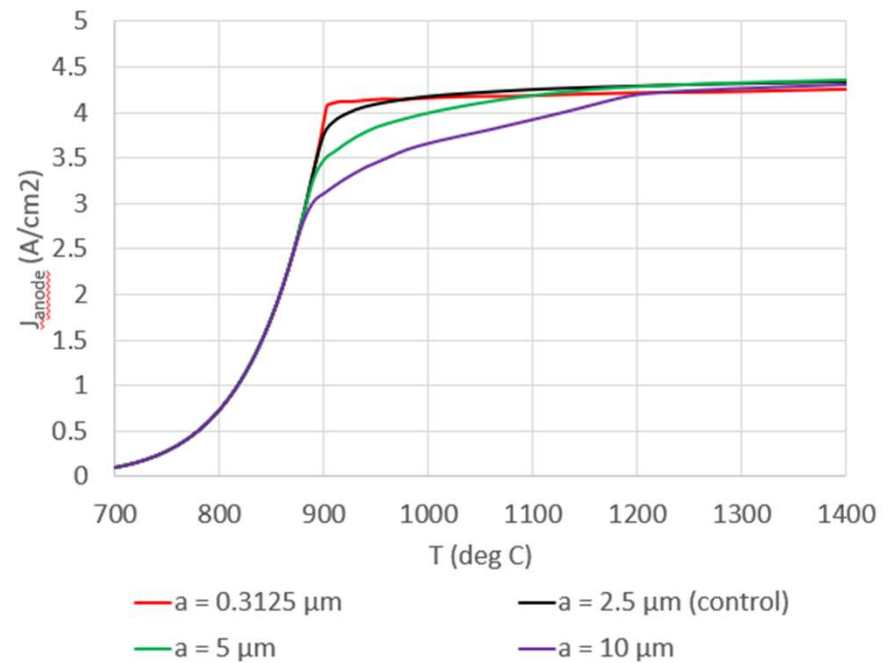
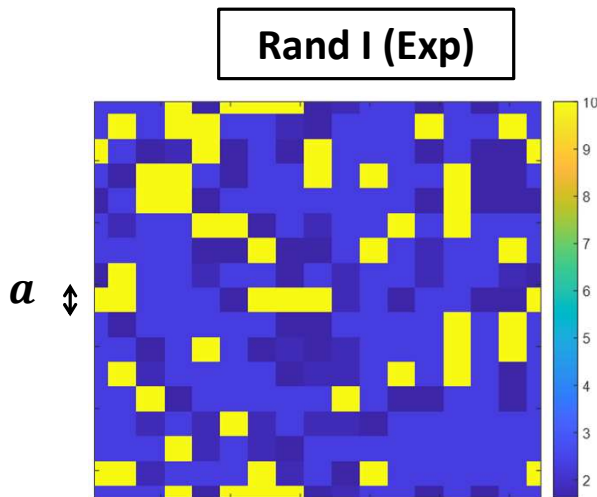
Work Function [eV]	Fractional cathode area in Rand I
1.61	17.97
1.79	9.77
2.3	9.38
2.31	43.75
10 (non-emitting)	19.14



2-1/2D Model [2]

Effect of tile size

- Smaller tile sizes correlate with sharper knees
- Comparison of $a = 0.3125 \mu\text{m}$ and $2.5 \mu\text{m}$ cases shows consistency with $K_3 = 0$ in the 3D CL law in the limit $a = 0$, and with the 2-1/2D model that employs realistic work function distributions.

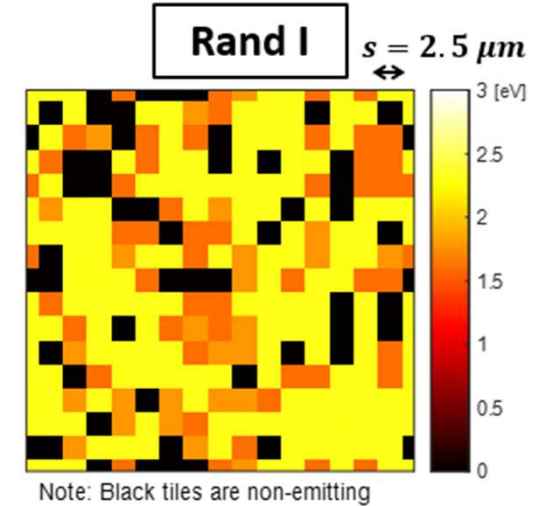
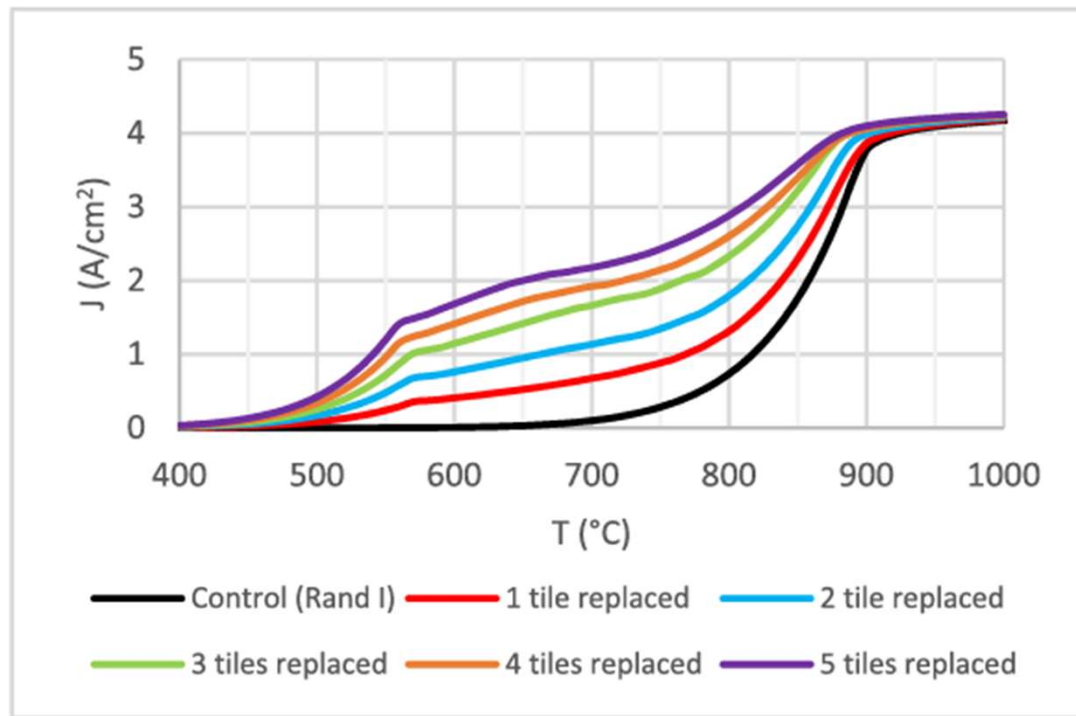


[2] A. Jassem, et al., IEEE Trans. Plasma Sci. 49, 749 (2021).

2-1/2D Model [2]



Effect of replacing increasing number of non-emitting tiles with local 'hotspots' (work function = 1 eV); to simulate surface roughness



[2] A. Jassem, D. Chernin, J. J. Petillo, Y. Y. Lau, A. Jensen, S. Ovtchinnikov, "Analysis of Anode Current From a Thermionic Cathode With a 2-D Work Function Distribution," IEEE Trans. Plasma Sci. 49, 749 (2021).



Conclusions on Miram curves

- Transverse electron motion is relatively unimportant to Miram curves (shape, smoothness, knee)
- With a sizable non-emitting region, the anode current is still governed by the 1D Child-Langmuir Law as if the entire cathode were emitting, at sufficiently high T_{cathode}
- Heavily emitting regions (regions of low work function) can make up large fraction of anode current as their neighboring non-emitting regions do not provide space charge shielding. This is purely a 2D – 3D effect
- Discrete work function distributions, randomly in both x and y , lead to smooth Miram curves
- Smaller emission (grain) size is correlated with sharper knees, at the same fraction of actively emitting areas
- Solving the reverse problem to determine work function distribution from a Miram curve is unlikely
- The 1D Child-Langmuir current density is a hard limit for the average current density over the entire cathode, regardless of the emission nonuniformity in space and in time ($Q \sim CV$)



What's new in the Ramo-Shockley Theorem?

Background: The Ramo-Shockley Theorem

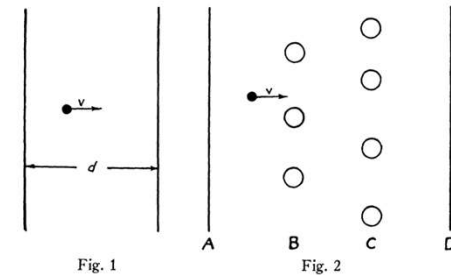


- A moving charge induces currents in nearby conductors, which was formulated by Ramo (1939) and Shockley (1938) [RS]
- Major assumptions in RS:
 - Charge motion is **nonrelativistic**.
 - Use only **electrostatic** fields.
- **New insights into:**
 - How do relativistic and electromagnetic effects modify RS, and possibly existing theories on multipactor discharge and high power microwave sources?

S. Ramo, Proc. IRE 27, 584 (1939)
 W. Shockley, J. Appl. Phys. 9, 635 (1938).

Currents Induced by Electron Motion

SIMON RAMO†, ASSOCIATE MEMBER, I.R.E.



Currents to Conductors Induced by a Moving Point Charge

W. SHOCKLEY
 Bell Telephone Laboratories, Inc., New York, N. Y.
 (Received May 14, 1938)

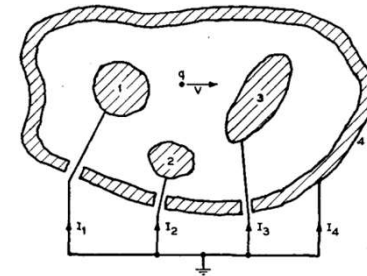
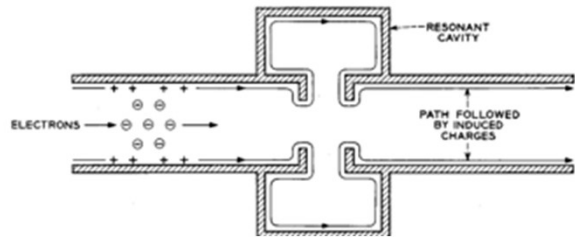
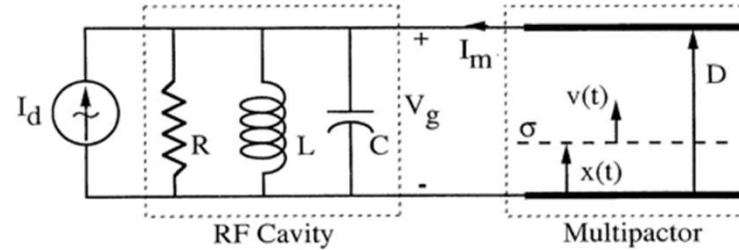


FIG. 1. Schematic representation of conductors and currents.

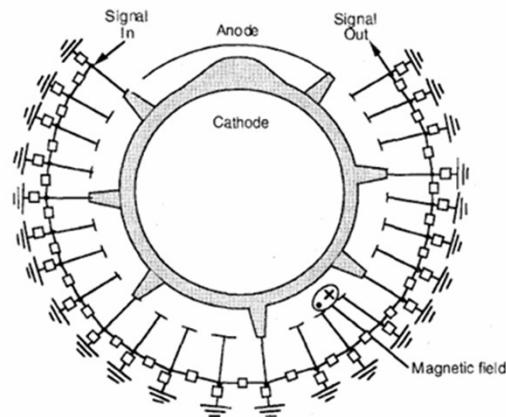
Induced Current Calculated from the Ramo-Shockley Theorem



**Excitation of klystron cavity
(from Gerwartowski and Watson)**



**Cavity loading by multipactor discharge
(from R. A. Kishek)**

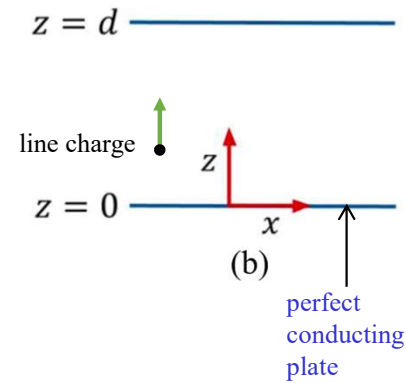


**Noise in crossed-field amplifier
(from D. Chernin)**

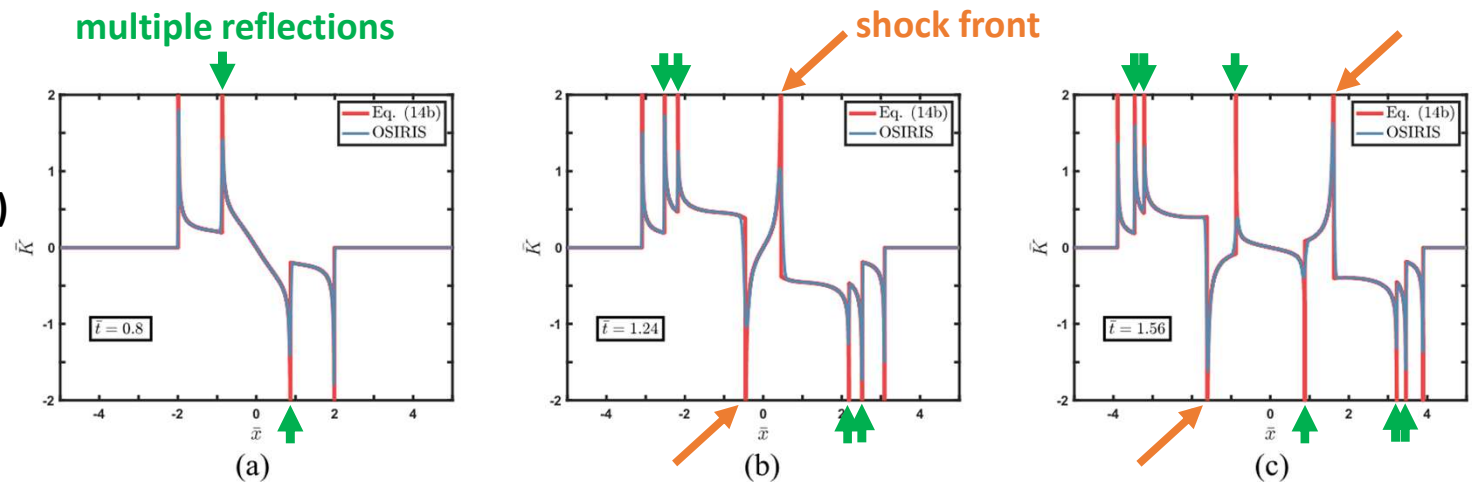
Extensions of Ramo-Shockley Theorem

Line charge strikes upper plate at $t = T$ and is removed, EM shock is formed, with closed form solution in Eq. (14b)

$$\bar{K}_x(x; t) = \begin{cases} \mathbf{K}(\bar{x}, \bar{t}, \bar{h}), & 0 < \bar{t} < \bar{T} & (14a) \\ \mathbf{K}(\bar{x}, \bar{t}, \bar{h}) - \mathbf{K}(\bar{x}, \bar{t} - \bar{T}, 1), & \bar{t} \geq \bar{T} & (14b) \end{cases}$$



Note almost perfect agreement between Eq. (14) and OSIRIS simulation results.



D. Li, D. Chernin, Y. Y. Lau, "A relativistic and electromagnetic correction to the Ramo-Shockley theorem," IEEE Trans. Plasma Sci. **49**, 2661 (2021).

D. Li, P. Wong, D. Chernin, and Y. Y. Lau, "Induced Current Due to Electromagnetic Shock Produced by Charge Impact on a Conducting Surface," IEEE Trans. Plasma Sci. **50**, 2838 (2022).

New Results on Ramo-Shockley Theorem



Discovered an electromagnetic shock when an electron strikes a conductor and is removed (a form of transition radiation), a phenomenon totally omitted in the classical Ramo-Shockley theorem.

Constructed closed form, simple analytic solutions which illustrate why RS works well in vacuum electronics (which ignores transients, multiple reflections, and electromagnetic shocks).

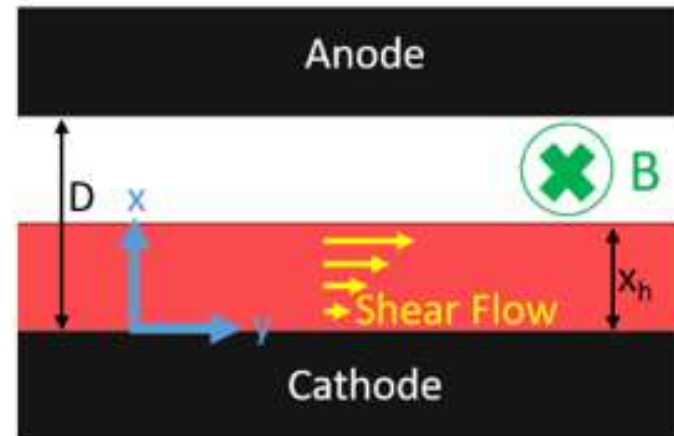
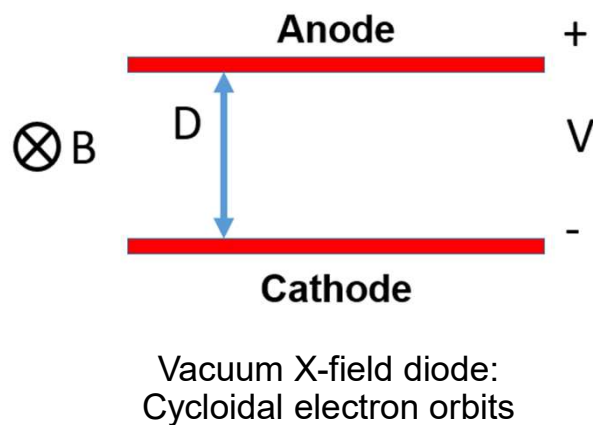
EM shock is unimportant to non-relativistic CFA's, magnetrons, and multipactor discharge because of low impact energy of electrons.

EM shock could provide additional beam loading in a relativistic magnetron or a magnetically insulated line oscillator (MILO) because of high impact energy of electrons. This is to be quantified.



What's new in Brillouin flow theory?

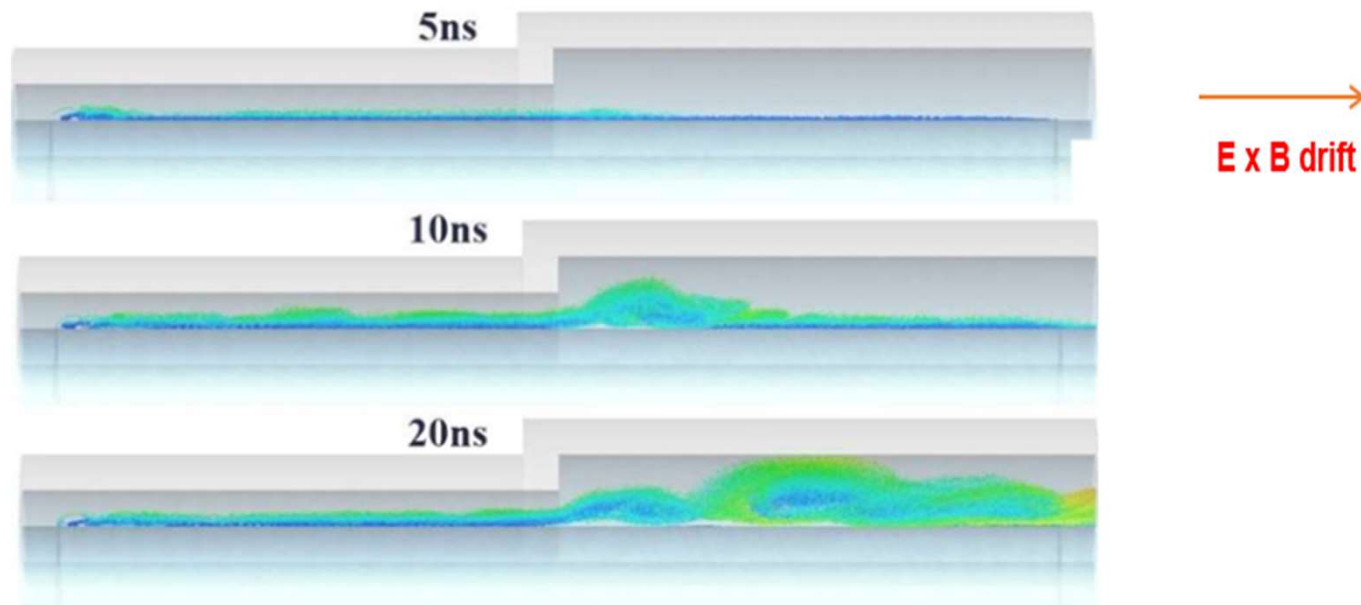
Crossed-Field Diodes



Both Slater and Buneman conjectured that the rectilinear electron shear flow (Brillouin flow with $\mathbf{E} = 0$ and $\mathbf{v} = 0$ on cathode) is the preferred state for magnetron, over the cycloidal orbit states.

Note: B may be provided by an external magnet (magnetron, relativistic magnetron), or by wall currents without an external magnet (MILO, MITL).

New Results*: Strong turbulence in 2-D Brillouin Flow Expanding into Wider Gap Region



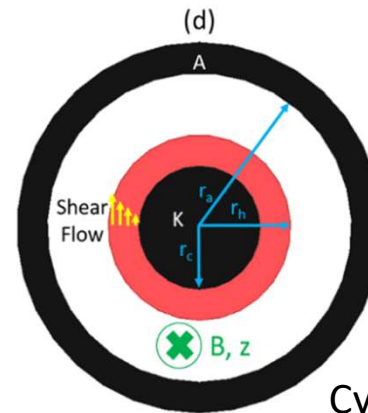
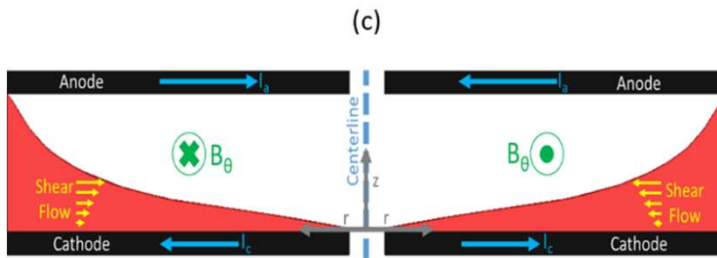
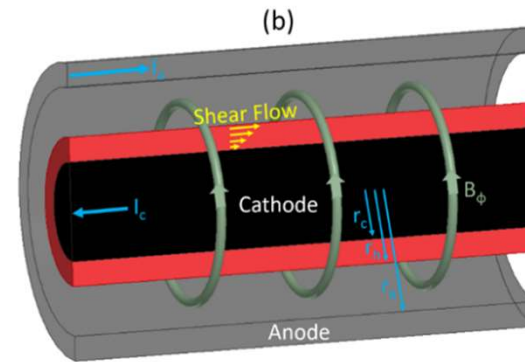
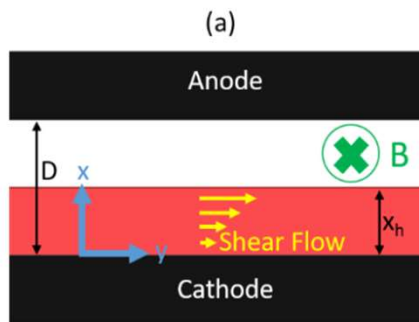
*R. A. Revolinsky, C. Swenson, N. Jordan, Y. Y. Lau, and R. M. Gilgenbach, "On the 2-dimensional Brillouin flow," arXiv:2404.11047; in this conference, Paper P6.9

Simple analytic solutions, and scaling laws, were derived for the Brillouin flow in four (4) classes of X-field devices



MITL, Planar magnetron,
MILO (Magnetically Insulated
Line Oscillator), and their hybrid

Cylindrical MILO
with axial electron flow



Cylindrical MITL with
radial electron flow

Cylindrical magnetron with
azimuthal electron flow



New insights into interesting questions [11] [12]:

- (a) Differences in operating mechanisms between magnetron and MILO?
- (b) Low voltage MILO?
- (c) Low current MILO?
- (d) Low impedance MILO driven by LTD
- (e) Optimal configuration in magnetron-MILO hybrid?

[11] Y. Y. Lau, D. A. Packard, C. J. Swenson, J. W. Luginsland, D. Li, A. Jassem, N. M. Jordan, R. D. McBride, and R. M. Gilgenbach, “Explicit Brillouin flow solutions in magnetrons, magnetically insulated line oscillators, and radial magnetically insulated transmission lines,” *IEEE Trans. Plasma Sci.* 49, 3418–3437 (2021).

[12] D. A. Packard, Y. Y. Lau, E. N. Guerin, C. J. Swenson, S. V. Langellotti, A. Jassem, D. Li, N. M. Jordan, J. W. Luginsland, R. D. McBride, and R. M. Gilgenbach, “Theory, simulation, and experiments on a magnetically insulated line oscillator (MILO) at 10 kA, 240 kV near Hull cutoff condition,” *Physics of Plasmas*, vol. 28, no. 12, p. 123102, (2021).

Some Open Questions



Why do RAN1, RAN2, RAN3 all conspire to converge to 1D CL at high T_{cathode} ?

Degree of beam-loading on MILO, MITL, and relativistic magnetron due to shock-induced current that was omitted in RS?

J(2D) and J(3D) for thermionic emission on a sheet beam and needle-like beam?

Crossed-field flows near Hull cutoff (transition between magnetic insulation and conduction)?

Plus the many “old” and “new” questions in Slide #1, some covered in this joint conference

Acknowledgements

**David Chernin, Kevin Jensen, John Petillo &
UM students and colleagues:**



Picture taken at ICOPS (2023, Santa Fe) on the retirement of Professors Ronald Gilgenbach and Y. Y. Lau